Discovering orbit and clock quality based on analysis

of wide-lane ambiguities derived from PPP models

Gang Chen [1], Sijing Liu [2,1],* and Qile Zhao [3],*

[1] China University of Geosciences, College of Maritime Science and Technology, Wuhan, 430074, China; ddwhcg@cug.edu.cn

[2] China University of Geosciences, Institute of Geophysics and Geomatics, Wuhan 430074, China; sijingliu@cug.edu.cn

[3] Wuhan University, GNSS Research Center, Wuhan 430079, China; zhaoql@whu.edu.cn

* Correspondence: sijingliu@cug.edu.cn; zhaoql@whu.edu.cn; Tel.: +0086-0270-15629083635

Abstract: Orbit and clock products are used in real-time GNSS precise point positioning without knowing their quality. This study develops a new approach to detect orbit and clock errors through comparing geometry-free and geometry-based wide-lane ambiguities in PPP model. The reparameterization and estimation procedures of the geometry-free and geometry-based ambiguities are described in detail. The effects of orbit and clock errors on ambiguities are given in analytical expressions. The numerical similarity and differences of geometry-free and geometry-based wide-lane ambiguities are analyzed using different orbit and clock products. Furthermore, two types of typical errors in orbit and clock are simulated and their effects on wide-lane ambiguities are numerically produced and analyzed. The contribution discloses that the geometry-free and geometry-based wide-lane ambiguities are equivalent in terms of their formal errors. Although they are very close in terms of their estimates when the used orbit and clock for geometry-based ambiguities are precise enough, they are not the same, in particular, in the case that the used orbit and clock, as a combination, contain significant errors. It is discovered that the discrepancies of geometry-free and geometry-based wide-lane ambiguities are coincided with the actual time-variant errors in the used orbit and clock at the line-of-sight direction. This provides a quality index for real-time users to detect the errors in real-time orbit and clock products, which potentially improves the accuracy of positioning.

Keywords: Geometry-free; geometry-based; wide-lane ambiguity; orbit and clock residual error

1. Introduction

Precise point positioning (PPP) using global navigation satellite systems measurements (GNSS) was initially proposed in [1] in order to solve the high computation burden of the network approach. The PPP technique employs only a single receiver to determine its position without explicitly using reference stations. To do so, precise orbit and clock are needed to enable absolute positioning of high accuracy [2]. This technique has been intensively developed from static to kinematic positioning [3], from post-processing to real-time service [4-5], form using GPS only to using multi-constellation systems [6], from ambiguity-float to integer ambiguity-fixed solution [7-10], from decimeter to centimeter accuracy [11]. The PPP technique has been started with the ionosphere-free combination approach [1] and then developed with the raw observation approach [11-15]. One of the major differences of these two approaches is that one eliminates the ionosphere delay while the other estimates it. Another main difference is that how to deal with the ambiguity parameter. The ambiguity term estimated with the ionosphere-free approach is actually a combination of narrow-lane (NL) and wide-lane (WL) ambiguity, while the raw observation approach produces L1 and L2 ambiguity parameters simultaneously together with the ionosphere term (let us consider only the case of dual frequencies). The common point for these two approaches is that their ambiguity

47 parameters do not have integer nature, as double-difference cannot be formed using a single receiver.
48 In this case, the satellite hardware delay cannot be separated or eliminated from the ambiguities in
49 the PPP mode. The term takes typically several tens of minutes to converge when the positioning
50 starts or resets after data interruption. The accuracy can be improved, and the convergence time can
51 be shortened if the ambiguities can be fixed correctly to their integers using additional corrections,
52 such as satellite phase biases.
53   A key task for the PPP integer ambiguity resolution is to separate or identify satellite phase
54 biases in the ambiguity term in the reference network and then to apply these biases to their
55 corresponding ambiguities in mobiles to restore integer nature [13-14]. The ionosphere-free approach
56 basically uses two parallel processes [7-10]. One process is to compute the geometry-free (GF) Hatch-
57 Melbourne-Wübbena combinations [16-18] in order to produce WL satellite phase biases and
58 integers. The other process is to carry out the geometry-based (GB) positioning to compute the
59 ionosphere-free ambiguity terms and further separate NL biases with involvement of integers of GF
60 WL ambiguities. The raw observation approach uses only one process that produces L1 and L2
61 ambiguities simultaneously [14], which are then used to form GB WL ambiguities and further
62 produce WL satellite phase biases. A variant of the raw observation approach is to produce WL and
63 L2 ambiguities simultaneously in the GB   model [15]. WL ambiguities are the basis of going forwards
64 for these two approaches. The difference is that one produces them with the GF model while the other
65 with the GB model. Then the question raises: are the GF WL ambiguities the same or equivalent with
66 the GB ones from even a single receiver in terms of estimates themselves and their formal precision?
67 The reason for such a question is to clear off the hesitation of mixing use of the corrections. That is to
68 say, if they are not the same or equivalent, one may hesitate to apply the GB WL corrections to the
69 ionosphere-free approach, or apply the GF WL corrections to the raw observation approach in user
70 side. The question has been positively answered in an analytical way in [19] using a between-satellite
71 single-difference functional model of multiple stations. However, there is no numerical analysis
72 based on the real data in literature. It concludes that the GF WL ambiguity precision does not differ
73 too much from its GB counterpart under an assumption of small to regional networks [19]. This
74 assumption does not consider the orbit and clock residual errors (i.e. the remaining error in precise
75 orbits and clocks as they are not perfect). Different questions may then raise. Do the orbit and clock
76 residual errors make differences for the GF and GB ambiguities? This is certainly not the case for the
77 GF ambiguities as the geometry related parameters, such as satellite/receiver positions,
78 satellite/receiver clock as well as troposphere delay, are eliminated. Then how about the GB
79 ambiguities? If so, in what level of orbit and clock quality, one could claim that the GF and GB
80 ambiguities are equivalent?
81   The quality of orbit and clock has been improved in the past years for post-processing products
82 [20] and real-time products [21]. The majority of GNSS community is producing real-time orbit and
83 clock step by step [5-6]. A set of satellite orbit parameters (initial state and solar radiation pressure)
84 is first determined using a network of globally distributed reference stations using the past 24 - 48
85 hours of GNSS measurements. The orbits of at least 3 hours are predicted using the obtained orbit
86 parameters. The predicted orbits are then used as input for clock bias filtering in which real-time
87 observations are used. The accuracy of the predicted orbit is dominated by the solar radiation
88 pressure [6]. In addition, the predicted orbit may not be precise enough in the eclipse and just out of
89 the eclipse seasons, due to the fact that the yaw attitude is not properly modelled. It is obvious that
90 the remaining error of predicted orbits with longer predict arc length could make significant negative
91 impact on the GB NL ambiguity estimation and integer resolutions [6]. Their impact on GB WL
92 ambiguities remains being not analyzed. Although it is possible to reduce the orbit error by
93 shortening the predict length, the variation of errors could be a couple of centimeters to decimeters.
94 There are also exceptional occasions that some satellites, like GPS IIF, could have large errors up to
95 meters in their predicted orbits [22]. These errors could significantly worsen the clock bias estimation
96 and satellite phase bias estimation as well as PPP integer ambiguity resolution in user side, in
97 particular for real-time users.

98   It is common to evaluate the quality of real-time orbit and clock by comparing them with the
99 post-processing counterpart separately [21]. However, the post-processing products are available
100 only after one day or a couple of hours later, which is not very acceptable for real-time users. In
101 addition, it is well known that the clock products absorb partly the errors of predicted orbits,
102 particularly errors of the line-of-sight (LOS) direction [23-25]. Therefore, it is more reasonable to
103 assess orbit and clock residual error as a whole directly from a user's perspective. The differences
104 between GF and GB wide-lane ambiguities is a starting point to investigate.
105   This contribution aims at analysis of single-site ambiguities derived from both GF and GB
106 model. We focus on numerical computation and analysis using raw observations without differential
107 and combination operator in the measurement domain. The GB WL ambiguities are derived using
108 different orbit and clock products. To simplify the presentation and discussion, we are focusing on
109 global positioning system (GPS) in this contribution, but this does not affect the generality of our
110 analysis for other constellations. We also investigate the discrepancies between GF and GB WL
111 ambiguities to disclose the orbit and clock quality from a user's perspective. The contribution is
112 arranged as follows: First, the GF and GB models are respectively presented in detail. Second, the
113 effects of orbit and clock errors on the ambiguities are given in an analytical way. Third, the results
114 of GB and GF ambiguities are numerically analyzed for both post-processing and real-time orbit and
115 clock products. In addition, we simulate two types of errors in orbit and clock and reprocess the data
116 and investigate the impact on WL ambiguities for further understanding. Finally, the study is
117 summarized with some conclusions.

2. WL ambiguities derived from the GF model

119   The observation equation for measurements of code p and phase φ tracked by a receiver at
120 location r from GPS satellites s $(s = 1, 2, \cdots, n)$, at frequency i $(i = 1, 2)$ at epoch k, can be
121 expressed in meters as follows:

$$E\{p_{i,r}^s(k)\} = \rho_r^s(k) + m_r^s \cdot T_r + \delta t_r(k) - \delta t^s(k) + \mu_i I_r^s(k) + d_{p_i,r} - d_{p_i}^s$$

$$E\{\varphi_{i,r}^s(k)\} = \rho_r^s(k) + m_r^s \cdot T_r + \delta t_r(k) - \delta t^s(k) - \mu_i I_r^s(k) + d_{\varphi_i,r} - d_{\varphi_i}^s + \lambda_i N_{i,r}^s \tag{1}$$

122 where $E\{\cdot\}$ denotes the expectation operator; $\rho_r^s(k)$ is the geometric range between the receiver
123 and satellite; T_r the zenith tropospheric delay with mapping function m_r^s; $\delta t_r(k)$ and $\delta t^s(k)$ the
124 receiver and satellite clock bias in meters, respectively; $\mu_i = \lambda_i^2 / \lambda_1^2$, λ_i the carrier wavelength of
125 frequency i; $I_r^s(k)$ the ionospheric delay; $d_{p_i,r}$ and $d_{\varphi_i,r}$ are the receiver hardware delays (or biases)
126 on code and phase, respectively; $d_{p_i}^s$ and $d_{\varphi_i}^s$ are the satellite hardware delays (or biases) on code and
127 phase, respectively; where it is assumed that these satellite hardware delays are relatively stable in
128 time; N_i the integer carrier ambiguity. All terms with (k) are supposed to be significantly changed
129 in time.
130   The so-called GF observation model dispenses with geometric a priori information. The
131 geometry part is obtained by combining all non-dispersive terms, δt^s including the geometric range
132 $\rho_r^s(k)$, satellite $\delta t^s(k)$ and receiver clock $\delta t_r(k)$ and tropospheric delay $m_r^s \cdot T_r$. Even though, the
133 system is rank deficient. Not all terms can be directly estimated. The hardware delays have to
134 distribute to other terms. Let us define the geometry part as one common term for all observations
135 from one satellite:

$$R_r^s(k) := \rho_r^s(k) + m_r^s \cdot T_r + \delta t_r(k) - \delta t^s(k) + \frac{\mu_2}{\mu_2 - \mu_1}(d_{p_1,r} - d_{p_1}^s) - \frac{\mu_1}{\mu_2 - \mu_1}(d_{p_2,r} - d_{p_2}^s) \tag{2}$$

136 and the ionosphere term is also combined with part of satellite and receiver hardware biases:

$$\widetilde{I}_r^s(k) := I_r^s(k) + \frac{\mu_1}{\mu_2 - \mu_1}(d_{p_2,r} - d_{p_2}^s - d_{p_1,r} + d_{p_1}^s) \tag{3}$$

137   and the *ambiguity* terms for L1 and L2 frequency are defined as:

$$\widetilde{N}_{i,r}^s := N_{i,r}^s + \frac{1}{\lambda_i}\left\{ d_{\varphi_i,r} - d_{\varphi_i}^s + \frac{\mu_i + \mu_1}{\mu_2 - \mu_1}(d_{p_2,r} - d_{p_2}^s) - \frac{\mu_i + \mu_2}{\mu_2 - \mu_1}(d_{p_1,r} - d_{p_1}^s) \right\}, \tag{4}$$

138   Therefore, the *functional GF model* is written as

$$E\{p_{i,r}^s(k)\} = R_r^s(k) + \mu_i\widetilde{I}_r^s(k)$$
$$E\{\phi_{i,r}^s(k)\} = R_r^s(k) - \mu_i\widetilde{I}_r^s(k) + \lambda_i\widetilde{N}_{i,r}^s \tag{5}$$

139   where the model is for a single satellite. Similar expressions can be seen in [19,27] with the single-
140   difference operator between satellites. Here, we focus on using raw measurements without any
141   difference and combination operator in observation domain. The epoch-wise solution of the
142   ambiguity term is simply computed as follows:

$$\mathbf{x}_k^s = \mathbf{H}\,\mathbf{z}_k^s \tag{6}$$

143   where the phase and code measurements can be written in a vector form as
144    $\mathbf{z}_k^s := \begin{bmatrix} p_{1,r}^s(k) & p_{2,r}^s(k) & \phi_{1,r}^s(k) & \phi_{2,r}^s(k) \end{bmatrix}^T$ and the parameters that we are interested is ambiguity term
145    $\mathbf{x}_k^s := \begin{bmatrix} \widetilde{N}_{1,r}^s & \widetilde{N}_{2,r}^s \end{bmatrix}^T$. $\mathbf{H}$ is the coefficient matrix derived from Equation (5) only for ambiguity
146   parameters. The ionosphere and geometry terms are eliminated, which is the origin that the term of
147   GF actually comes from.
148   The stochastic model for the observation is given as follows:

$$\mathbf{Q}_{\mathbf{z}_k^s} = diag\{\sigma(e)_p^2, \sigma(e)_p^2, \sigma(e)_\phi^2, \sigma(e)_\phi^2\} \tag{7}$$

149   where *e* is the elevation. According to the *error propagation law*, the variance-covariance of ambiguity
150   terms can be derived as:

$$\mathbf{Q}_{\mathbf{x}_k^s} = \mathbf{H}\mathbf{Q}_{\mathbf{z}_k^s}\mathbf{H}^{\mathbf{T}} \tag{8}$$

151   where Equations (6) and (8) are used to compute the epoch-wise L1 and L2 ambiguities and their
152   variance-covariance. However, the epoch-wise solution has no redundancy. The solution is rather
153   noisy as it is purely dominated by noise of code measurements. To increase the accuracy, an
154   averaging filter is implemented using multi-epoch solutions in a recursive way. Let us notate the
155   averaging solution as follows:

$$\hat{\mathbf{x}}_k^s := \begin{bmatrix} \hat{\widetilde{N}}_{1,r}^s & \hat{\widetilde{N}}_{2,r}^s \end{bmatrix}^T \tag{9}$$

156   and the averaging filter starts at epoch 1 as $\hat{\mathbf{x}}_1^s = \mathbf{x}_1^s$ and $\mathbf{Q}_{\hat{\mathbf{x}}_1^s} = \mathbf{Q}_{\mathbf{x}_1^s}$.

157   Assume that the filtering solution at the epoch k-1 is denoted as $\hat{\mathbf{x}}_{k-1}^s$ with its covariance matrix
158    $\mathbf{Q}_{\hat{\mathbf{x}}_{k-1}^s}$, the variance-covariance is first updated with the assumed process noise for epoch solution at
159   k:

$$\mathbf{Q}_{\hat{\mathbf{x}}_{k,k-1}^s} = \mathbf{Q}_{\hat{\mathbf{x}}_{k-1}^s} + \mathbf{Q}_{\mathbf{w}} \tag{10}$$

160   where, $\mathbf{Q}_{\mathbf{w}}$ is computed from the assumed process noise multiplying with time interval between
161   epoch k and k-1, and then updated with the epoch-wise variance-covariance

$$\mathbf{Q}_{\hat{\mathbf{x}}_k^s} = (\mathbf{Q}_{\hat{\mathbf{x}}_{k,k-1}^s}^{-1} + \mathbf{Q}_{\mathbf{x}_k^s}^{-1})^{-1} \quad , \tag{11}$$

162   with the parameter being also updated with the epoch-wise estimate and its variance-covariance

$$\hat{\mathbf{x}}_k^s = \hat{\mathbf{x}}_{k-1}^s + \mathbf{Q}_{\hat{\mathbf{x}}_k^s}\mathbf{Q}_{\mathbf{x}_k^s}^{-1}(\mathbf{x}_k^s - \hat{\mathbf{x}}_{k-1}^s) \quad , \tag{12}$$

163   where elements of $\hat{\mathbf{x}}_k^s$ and $\mathbf{Q}_{\hat{\mathbf{x}}_k^s}$ are used to derive the WL ambiguity, i.e.

$$\hat{\tilde{N}}_{wl,r}^s = \hat{\tilde{N}}_{1,r}^s - \hat{\tilde{N}}_{2,r}^s \,, \tag{13}$$

164   with its formal error being derived

$$\sigma_{\hat{\tilde{N}}_{wl,r}^s} = \sqrt{\sigma_{\hat{\tilde{N}}_{1,r}^s}^2 + \sigma_{\hat{\tilde{N}}_{2,r}^s}^2 - 2\cdot\sigma_{\hat{\tilde{N}}_{1,r}^s,\hat{\tilde{N}}_{2,r}^s}} \,, \tag{14}$$

165   where $\sigma_{\hat{\tilde{N}}_{1,r}^s}^2, \sigma_{\hat{\tilde{N}}_{2,r}^s}^2, \sigma_{\hat{\tilde{N}}_{1,r}^s,\hat{\tilde{N}}_{2,r}^s}$ are taken from $\mathbf{Q}_{\hat{\mathbf{x}}_k^s}$.

3. WL ambiguities derived from the GB model

167   To derive the ambiguities from the GB model, we assume that the station coordinates
168   (X_r, Y_r, Z_r), satellite orbit $(X^s(k), Y^s(k), Z^s(k))$ and clock errors $\delta t_{if}^s(k)$ are precisely known. As we
169   know that the satellite clock errors are calculated from ionosphere-free combination observations [2]:

$$\delta t_{if}^s(k) = \delta t^s(k) + \frac{\mu_2}{\mu_2 - \mu_1}d_{p_1}^s - \frac{\mu_1}{\mu_2 - \mu_1}d_{p_2}^s \,, \tag{15}$$

170   and the computed range between satellite and the known station coordinates is

$$\rho_r^s(k) = \sqrt{\{X^s(k) - X_r\}^2 + \{Y^s(k) - Y_r\}^2 + \{Z^s(k) - Z_r\}^2}$$

171

172   Add Equation (15) to Equation (1), insert $\rho_r^s(k)$ the left side, and define the observed minus
173   computed values as:

$$\delta p_{i,r}^s(k) := p_{i,r}^s(k) - \rho_r^s(k) + \delta t_{if}^s(k)$$
$$\delta \varphi_{i,r}^s(k) := \varphi_{i,r}^s(k) - \rho_r^s(k) + \delta t_{if}^s(k) \quad , \tag{16}$$

174   resulting in the following:

$$E\{\delta p_{i,r}^s(k)\} = m_r^s T_r + t_r(k) + \mu_i \tilde{I}_r^s(k)$$
$$E\{\delta \varphi_{i,r}^s(k)\} = m_r^s T_r + t_r(k) - \mu_i \tilde{I}_r^s(k) + \lambda_i \tilde{N}_{i,r}^s \quad , \tag{17}$$

175   Where the ionosphere and ambiguity terms are defined as the same as in Equations (3) and (4),
176   respectively, and the receiver clock term is defined as:

$$t_r(k) := \delta t_r(k) + \frac{\mu_2}{\mu_2 - \mu_1}d_{p_1,r} - \frac{\mu_1}{\mu_2 - \mu_1}d_{p_2,r}$$

177

178   The observation equations of all observed satellites in the matrix-vector form can be expressed
179   as:

$$\mathbf{y}_k = \mathbf{A}_k \tilde{\mathbf{x}}_k + \boldsymbol{\varepsilon} \,, \tag{18}$$

180   where $\tilde{\mathbf{x}}_k := \begin{bmatrix} T_r & t_r(k) & \mathbf{I}_r(k) & \mathbf{N}_{1,r} & \mathbf{N}_{2,r} \end{bmatrix}^T$ with $\mathbf{I}_r(k) := \begin{bmatrix} \tilde{I}_r^1(k) & \tilde{I}_r^2(k) & \cdots & \tilde{I}_r^m(k) \end{bmatrix}^T$ and

181    $\mathbf{N}_{i,r}(k) := \begin{bmatrix} \tilde{N}_{i,r}^1 & \tilde{N}_{i,r}^2 & \cdots & \tilde{N}_{i,r}^m \end{bmatrix}^T$, $\mathbf{y}_k := \begin{bmatrix} \mathbf{P}_{1,r} & \mathbf{P}_{2,r} & \Phi_{1,r} & \Phi_{2,r} \end{bmatrix}^T$ with $\mathbf{P}_{i,r} := \begin{bmatrix} \delta p_{i,r}^1 & \delta p_{i,r}^2 & \cdots & \delta p_{i,r}^m \end{bmatrix}^T$ and

182    $\Phi_{i,r} := \begin{bmatrix} \delta\varphi_{i,r}^1 & \delta\varphi_{i,r}^2 & \cdots & \delta\varphi_{i,r}^m \end{bmatrix}^T$; $\mathbf{A}_k$ is the design matrix with its elements being formed with the
183   coefficients in Equation (17) for all visible satellites.
184   The stochastic model is expressed as :

$$\boldsymbol{\varepsilon} \sim N(0, \mathbf{Q}_{\mathbf{y}_k}) , \tag{19}$$

185   where $\mathbf{Q}_{\mathbf{y}_k} = diag\{\sigma(e)_p^2 \quad \sigma(e)_p^2 \quad \cdots \quad \sigma(e)_p^2 \quad \sigma(e)_\phi^2 \quad \sigma(e)_\phi^2 \quad \cdots \quad \sigma(e)_\phi^2\}$.

186   It is noticed that the observation equation (18) has redundancy when the number of satellites is
187   larger than three, which is easy to achieve even when only GPS satellites are employed. The state
188   transition equation is given by

$$\widetilde{\mathbf{x}}_k = \mathbf{B}\widetilde{\mathbf{x}}_{k-1} + \mathbf{w} , \tag{20}$$

189   where $\mathbf{B} := \begin{bmatrix} 1 & 0 & \mathbf{0}_m^T & \mathbf{e}_m^T & \mathbf{e}_m^T \end{bmatrix}^T$ with $\mathbf{w} \sim N(0, \mathbf{Q}_\mathbf{w})$ which links that the troposphere and ambiguity
190   parameters with that of previous epochs.
191   Assume that the filtering solution at the epoch k-1 is denoted as $\hat{\widetilde{\mathbf{x}}}_{k-1}$ with its covariance matrix
192    $\mathbf{Q}_{\hat{\widetilde{\mathbf{x}}}_{k-1}}$, the solution at the epoch k is computed as:

$$\hat{\widetilde{\mathbf{x}}}_k = \hat{\widetilde{\mathbf{x}}}_{k,k-1} + \mathbf{K}_k(\mathbf{y}_k - \mathbf{A}_k\hat{\widetilde{\mathbf{x}}}_{k,k-1}), \tag{21}$$

193   with its covariance matrix being computed as

$$\mathbf{Q}_{\hat{\widetilde{\mathbf{x}}}_k} = (\mathbf{I} - \mathbf{K}_k\mathbf{A}_k)\mathbf{Q}_{\hat{\widetilde{\mathbf{x}}}_{k,k-1}} , \tag{22}$$

194   where $\hat{\widetilde{\mathbf{x}}}_{k,k-1} = \mathbf{B}\hat{\widetilde{\mathbf{x}}}_{k-1}$, and its covariance matrix as $\mathbf{Q}_{\hat{\widetilde{\mathbf{x}}}_{k,k-1}} = \mathbf{B}\mathbf{Q}_{\hat{\widetilde{\mathbf{x}}}_{k-1}}\mathbf{B}^T + \mathbf{Q}_\mathbf{w}$, and the gain matrix is computed
195   as $\mathbf{K}_k = \mathbf{Q}_{\hat{\widetilde{\mathbf{x}}}_{k,k-1}}\mathbf{A}_k^T(\mathbf{A}_k\mathbf{Q}_{\hat{\widetilde{\mathbf{x}}}_{k,k-1}}\mathbf{A}_k^T + \mathbf{Q}_{\mathbf{y}_k})^{-1}$.

196   The L1 and L2 ambiguities with their covariance matrix can be used to derive the GB WL
197   ambiguity and its formal error as Equations (13) and (14) for their GF counterparts.

4. Impact of orbit and clock residual errors on ambiguity estimation

199   From Equations (5) and (17), there is no difference between the GF and GB ambiguities in terms
200   of parameterization. However, their estimates are different since they go through different estimation
201   procedures. For the GF ambiguities, the geometry related terms, including orbit and clock, are
202   eliminated without effects. However it results in no redundancy for the epoch-wise estimates. The
203   solution's accuracy is dominated by the noise of code measurements. In this case, the solution with
204   multiple epochs is computed. For the GB ambiguities, the geometry strength is higher (as there are
205   redundancy in each epoch), the ambiguities converge quicker than the GF ones. However, the
206   observed minus computed values are computed from the orbit and clock, which are not always
207   precise enough. The orbit and clock residual error at the LOS remains in the observation as follows:

$$\begin{aligned} E\{\delta p_{i,r}^s(k)\} &= m_r^s T_r + t_r(k) + \mu_i \widetilde{I}_r^s(k) + oc_r^s \\ E\{\delta\varphi_{i,r}^s(k)\} &= m_r^s T_r + t_r(k) - \mu_i \widetilde{I}_r^s(k) + \lambda_i \widetilde{N}_{i,r}^s + oc_r^{s'} \end{aligned} \tag{23}$$

208   where oc_r^s indicates the slowly time-variant or time-invariant residual part of orbit and clock error
209   combination in the LOS direction. As they are not random noise, they could be distributed to every
210   parameters (as well as measurement residuals), but most likely to the ionosphere and ambiguity
211   terms of the satellite as these parameters are satellite dependent. There are two cases worthy of
212   investigation.

4.1. Orbit and clock residual error being constant bias

214   It is possible that the orbit and clock contain a constant bias. For example, the code measurement
215   type used in mobile side is not consistent with the code measurements used in the reference side

216 when computing the clock products. Assuming that the oc_r^s is a constant during the whole
217 measurement period and there are no effects on and from another satellites. As phase measurements
218 are assigned much higher weight than code ones (100 times smaller in terms of standard deviation),
219 we assume no significant orbit and clock errors are attributed to phase measurement residuals.
220 Furthermore, the ambiguities are common terms between epochs, they likely absorb the constant bias
221 as:

$$
\begin{aligned}
\widetilde{\widetilde{N}}_{1,r}^s &:\approx \widetilde{N}_{1,r}^s + \frac{1}{\lambda_1}\frac{\mu_1 + 3\mu_2}{2\mu_2}\, oc_r^s \ , \\
\widetilde{\widetilde{N}}_{2,r}^s &:\approx \widetilde{N}_{2,r}^s + \frac{1}{\lambda_2}\frac{3\mu_1 + \mu_2}{2\mu_1}\, oc_r^s
\end{aligned}
\tag{24}
$$

222 The remaining error may be distributed to the ionosphere term and the code residuals. From the
223 analytical expression of Equation (24), the effect on the WL ambiguity term is less than one tenth of
224 oc_r^s in terms of cycle. In other words, the effect of constant bias in orbit and clock looks largely
225 reduced. Bearing in mind that the reality can be more complex when our assumptions do not hold
226 for all cases. In particular, the geometry changing may have influence as well. However, the effects
227 of a constant bias analyzed here might be a minimum (i.e. a bottom line).

4.2. Orbit and clock residual error being time-variant error

229 The residual orbit and clock error is rarely a constant bias in an entire tracking period, except for
230 a mixture use of code measurements. It is very likely a time variant error that caused by the changes
231 of LOS and the orbit error itself (as will be shown later). In this case, it is not a trivial to make a strict
232 analytical expression, as the estimation procedure is rather complex both in current epoch and
233 correlation between epochs. Assume that the error is directly mapped to the ambiguity terms as
234 follows:

$$
\begin{aligned}
\widetilde{\widetilde{N}}_{1,r}^s &:\approx \widetilde{N}_{1,r}^s + \frac{1}{\lambda_1}\, oc_r^s \ , \\
\widetilde{\widetilde{N}}_{2,r}^s &:\approx \widetilde{N}_{2,r}^s + \frac{1}{\lambda_2}\, oc_r^s
\end{aligned}
\tag{25}
$$

235 where the effect on WL ambiguity term will be about $1.165 \cdot oc_r^s$ cycle. In other words, one meter bias
236 could bring 1.165 cycle error into the WL ambiguity. Even when the error is about 15 cm (often the
237 case for real-time orbit and clock), the effects will be significantly up to 0.18 cycle, which is not
238 acceptable for phase bias calibration for PPP IAR. In reality, the effects might be around (larger or
239 smaller than) this level due to different geometry strength. This contribution will make a real-data
240 numerical analysis in order to further understand the effects.

5. Experiment and results analysis

242 In order to analyze the performance of GF and GB WL ambiguities and evaluate the orbit and
243 clock effects on the WL ambiguities, we implemented the GF and GB models using raw observations
244 to compute L1, L2 and WL ambiguities as well as their variance-covariance as described in "WL
245 ambiguities derived from the GF model" and "WL ambiguities derived from the GB model". GNSS
246 measurements with 1 second interval from selected IGS sites are downloaded from the IGS data base.
247 These sites are deliberately selected and spread over main continents and the middle of the Pacific in
248 terms of groups, see Figure 1. Some of groups have sites located at very nearby in order to have
249 almost the same LOS. Two types of orbit and clock products are used in the experiment. One type is
250 the determined orbit and clock products provided by ESA to the IGS, while the other is the real-time
251 orbit and clock estimated as described in [15]. The interval of satellite orbit is 15 min, and the sample
252 rate of satellite clock is 30 s for both types of products. The determined products are obtained by the
253 post-processing mode, and their accuracy is better than that of real-time ones [15]. The standard GB
254 PPP solutions, in parallel with the GF process, are computed using raw L1 and L2 observations. The
255 parameters to be estimated are tropospheric zenith delay, ionosphere, receiver clock bias, and L1, L2

256   and then WL ambiguity terms for the GB process, while the GF process just produces the L1, L2 and
257   then WL ambiguity terms. The positions of sites are fixed to the "ground truth", which are computed
258   from many days' data with the static mode. The orbit and clock are integrated and interpolated for
259   each epoch (1 s of data interval). Strictly speaking, the interpolation for real-time orbit and clock is
260   not realistic in the real-time application as the future correction stream cannot be known in advance
261   for interpolation of current epoch. However, we employ exactly the same process in order to carry
262   out a fair comparison for both types of products by ignoring correction age effects. The elevation-
263   dependent data weighting is used for both processes. The entire process is implemented through a
264   strictly forward computation.

265
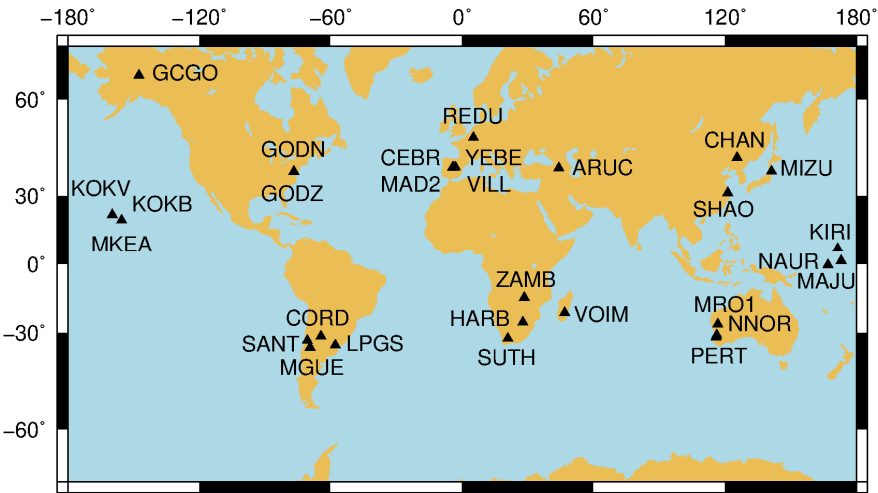
266   **Figure 1.** Distribution of sites that are used for this study

267   *5.1. Analysis of GB and GF ambiguities*

268   This section will analyze the GB and GF ambiguities and inspect the similarity and discrepancies
269   of GB and GF WL ambiguities.
270   Figure 2 shows the comparison of L1, L2 and WL ambiguities and their corresponding formal
271   standard deviations of PRN 09 produced with the GF and GB models for site CEBR. Arbitrary offsets
272   are removed from these ambiguities. It is obvious that both the variation of GF ambiguities and their
273   formal errors are larger than the GB counterparts, and especially they converge much slowly than
274   that of GB. However, as for WL ambiguities, the precisions are very consistent and they are almost
275   the same, meanwhile their estimates reveal a consistent trend despite of some small fluctuations. This
276   confirms the analytical statement in [19] that the GF WL ambiguity precision does not differ too much
277   from its GB counterpart. The reason is that the GF L1 and L2 ambiguities are highly correlated and
278   even more correlated than that of GB ones. The WL ambiguities are therefore much precise after the
279   differential operator, referring to (13)-(14), compared with the L1 and L2 ones. It is noticed that the
280   GF WL ambiguities are slightly oscillated, compared with the GB ones at the first hour, but they are
281   even stable than the GB ones afterwards. The reason is that the GB WL ambiguities may suffer some
282   errors in orbit and clock. This will be further analyzed in other sections.
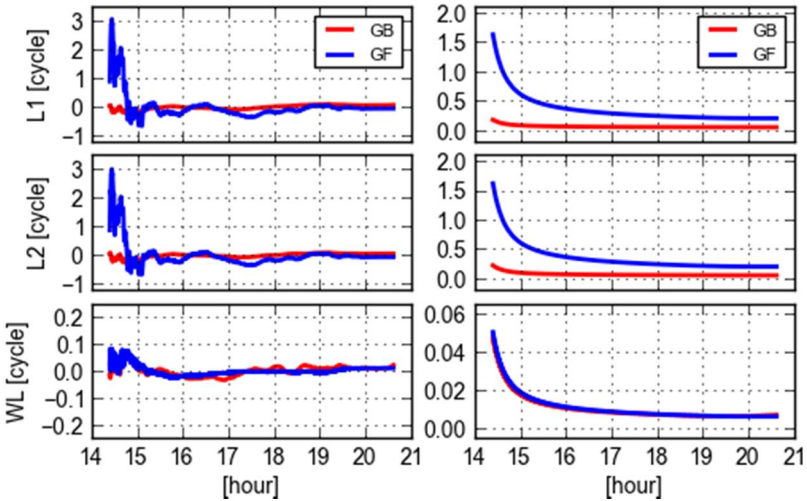
Figure 2. GF (blue) and GB (red) L1, L2 and WL ambiguities (left) and their corresponding formal errors (right) of PRN 09 computed from a single receiver (CEBR) observations and ESA final orbit and clock products

As can be seen from Figure 3 that the results of PRN 09 computed by another single receiver REDU have similar behavior to that of CEBR, which indicates that the WL ambiguities and their formal errors have commonality for this same satellite obtained by different receivers which are located not very far away.
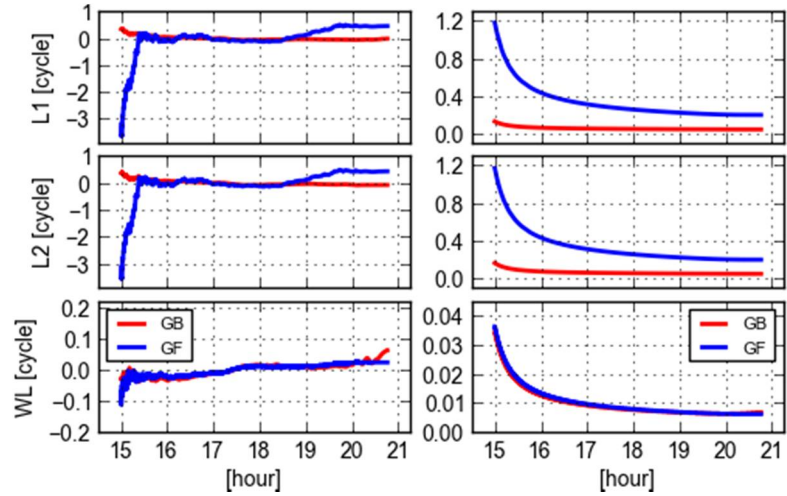
Figure 3. GF (blue) and GB (red) L1, L2 and WL ambiguities (left) and their corresponding formal errors (right) of PRN 09 computed using a single receiver (REDU) observations and ESA final orbit clock products

Figure 4 displays the differences of GB and GF WL ambiguities and their computed standard deviations derived from GB and GF ones using the error propagation law for PRN 09 at the site CEBR and REDU, respectively. The values of GB-GF are stably in between ± 0.1 cycles. The variation at the first hour is largely dominated by the GF ambiguities, while it changes due to the variation of GB ambiguities afterwards. The variations of GB-GF values are mostly within three times of the formal errors, which indicates that the formal errors statistically reflect the level of quality.
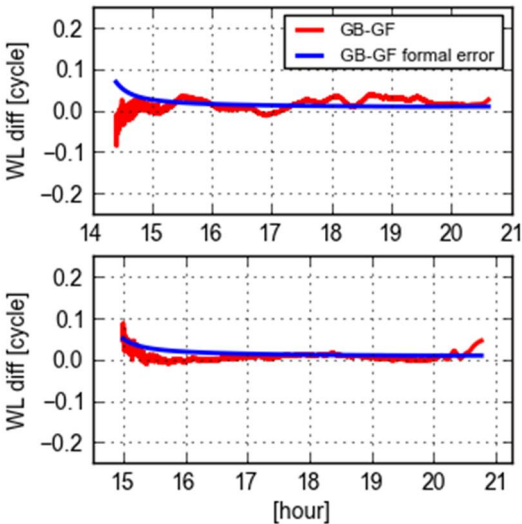
Figure 4. Differences of GB and GF WL ambiguities (red) and their formal errors (blue) of PRN 09 from the receivers CEBR (top) and REDU (bottom).

Figure 5 displays the values of GB-GF WL ambiguities computed with ESA final orbit and clock products at site KOKV for all visible GPS satellites. It is seen that these values are stable and close to zero. Again, the typical behavior of these time series is that they are noisy at the beginning of a tracking period, but become smooth and stable afterwards. According to the statistics, the biases are smaller than 0.05 cycle and the standard deviations of these values are smaller than 0.025 cycle. It is practically and commonly believed that the repeatability is good enough if differences of ambiguities are smaller than 0.1 cycle [7]. Therefore, we could state that the GB and GF WL ambiguities are equivalent in this case, though they are not the same.
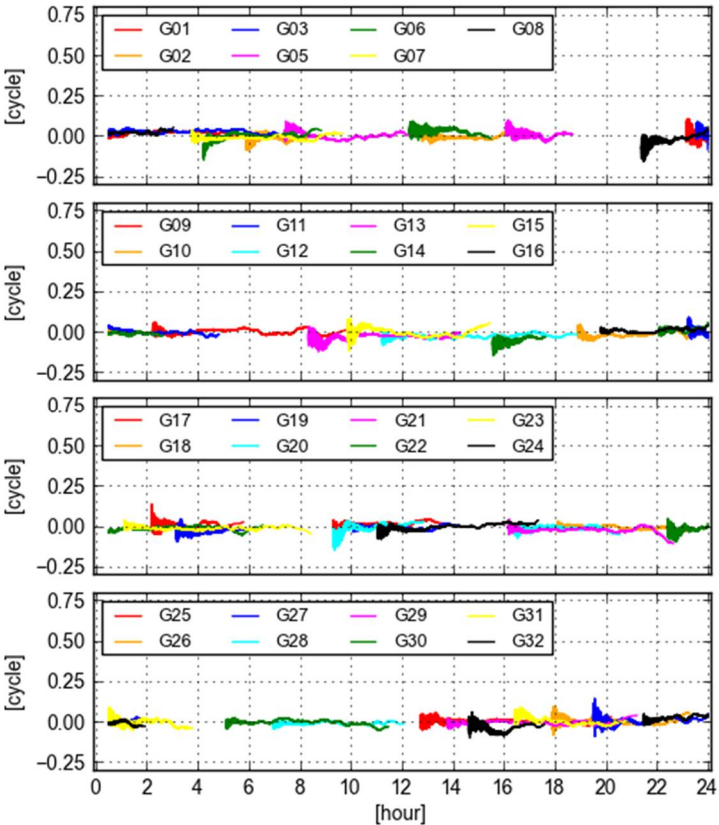
313   **Figure 5.** Differences of GB and GF WL ambiguities computed with ESA final orbit and clock products
314   at site KOKV

315   *5.2. Orbit and clock residual error effects*

316   The results demonstrated in previous section are computed with the ESA final orbit and clock
317   products. To compare with them, this section will show results that are computed with the real-time
318   orbit and clock products.
319   Figure 6 displays various differences of PRN 09 WL ambiguities and orbit clock products
320   computed at the site CEBR and REDU, respectively. In top panels, the GF WL differences are zeros
321   as the orbit and clock are eliminated and have no impact on the GF ambiguity estimates. The GB WL
322   differences are computed with final and real-time orbit and clock. In this case, everything is the same
323   except that the orbit and clock used are different. Therefore, the GB WL differences indicate that the
324   effects of the different orbit and clock products. To further confirm this, the differences of two types
325   of orbit and clock are also computed for the locations of the receivers, in which the orbits are mapped
326   into the LOS direction. The values are converted to cycles by divided with the wavelength of WL
327   ambiguities (which is 86.2 cm). It is clear that the variations of two sets of orbit and clock differences
328   are largely coincide with the differences of GB WL ambiguities.   In bottom panels, the GB minus GF
329   WL ambiguities used two types of orbit and clock products are shown together with the orbit and
330   clock differences themselves. The values of GB-GF computed from the final orbit and clock (OC1:
331   GB-GF in the figure) are more stable than that of computed from the real-time orbit and clock (OC2:
332   GB-GF in the figure). The latter one has a clear slope in the time series, which is consistent with the
333   slope of orbit and clock differences. In this case, it is difficult to say the GF WL ambiguities are
334   equivalent with the GB ones. However, it is promising for the real-time users that the GB-GF WL
335   ambiguities can be used to an indicator of the orbit and clock quality from a user's perspective.

336
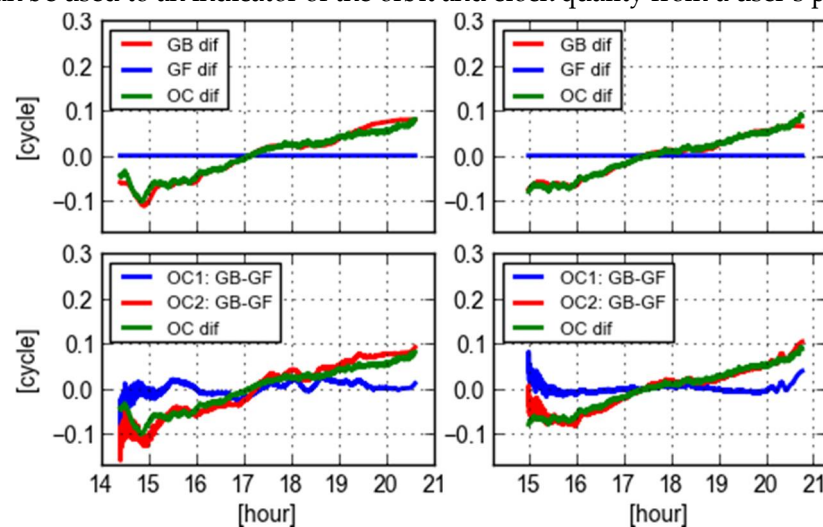
337   **Figure 6.** Various differences of PRN 09 WL ambiguities and orbit clock products computed at the
338   receiver CEBR (left) and REDU (right): 1) differences of GB ambiguities computed with final and real-
339   time orbit clock products are indicated in red in top panels; 2) differences of GF ambiguities computed
340   with final and real-time orbit clock products are indicated in blue in top panels; 3) differences of GB
341   and GF ambiguities computed with final orbit clock products (OC1) are indicated in blue in bottom
342   panels; 4) differences of GB and GF ambiguities computed with real-time orbit clock products (OC2)
343   are indicated in red in bottom panels; 5) differences of orbit clock impacts in LOS directions between
344   final and real-time orbit clock products in green

345   Figure 7 displays the values of GB - GF WL ambiguities computed with real-time orbit and clock
346   products at site KOKV for all visible GPS satellites. During the period of 2-12 O'clock, the variations
347   of these time series are larger than the rest of day. In particular, the largest variation is from PRN 09,
348   which is even larger than 1.0 cycle during 9-10 O'clock. The bias and the standard deviation are -0.569

349   and 0.305 cycle according to the statistics. In this case, the GB and GF WL ambiguities are not
350   equivalent.
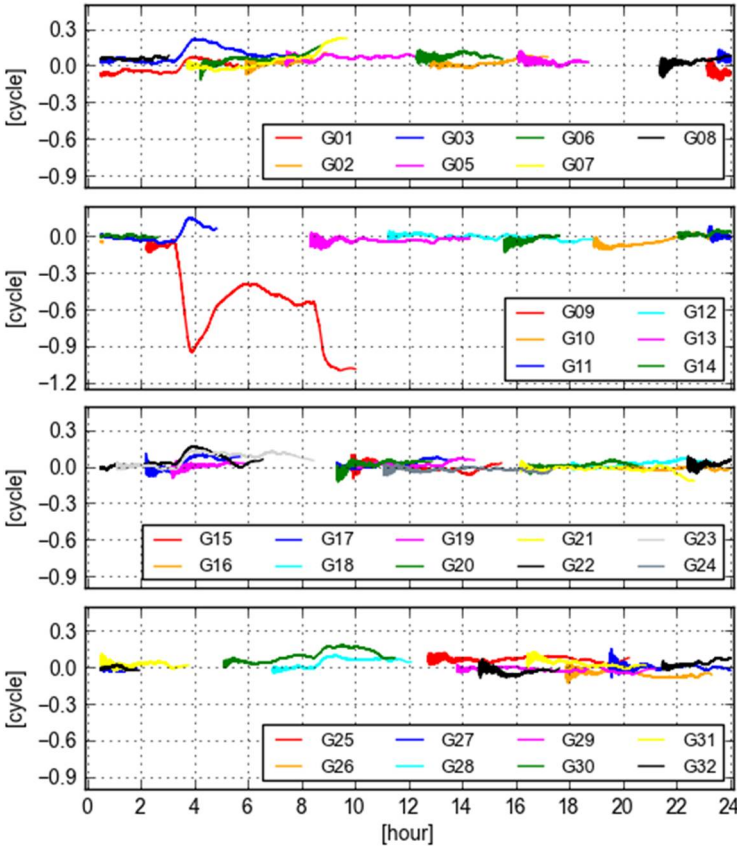
Figure 7. Differences of GB - GF WL ambiguities computed with real-time orbit and clock products
at Site KOKV

354   To further investigate the cause of the variation in GB-GF WL ambiguities, we plot the variations
355   of differences between the final and real-time orbit clock (orbit is projected into the LOS) at Site KOKV
356   for all visible GPS satellites in figure 8. It is clearly seen that the pattern of the orbit and clock
357   differences is very similar with that of GB-GF ambiguities, in particular, for the satellite PRN 09. The
358   reason for such an extreme orbit and clock behavior in real-time is likely that the orientation of the
359   satellite (mainly IIF satellites) is estimated or predicted wrongly [22]. This issue has not been solved
360   in real-time case. Therefore, it is valuable that the variation of GB-GF values of a receiver can be taken
361   as a quality index of orbit clock products from users' perspective.
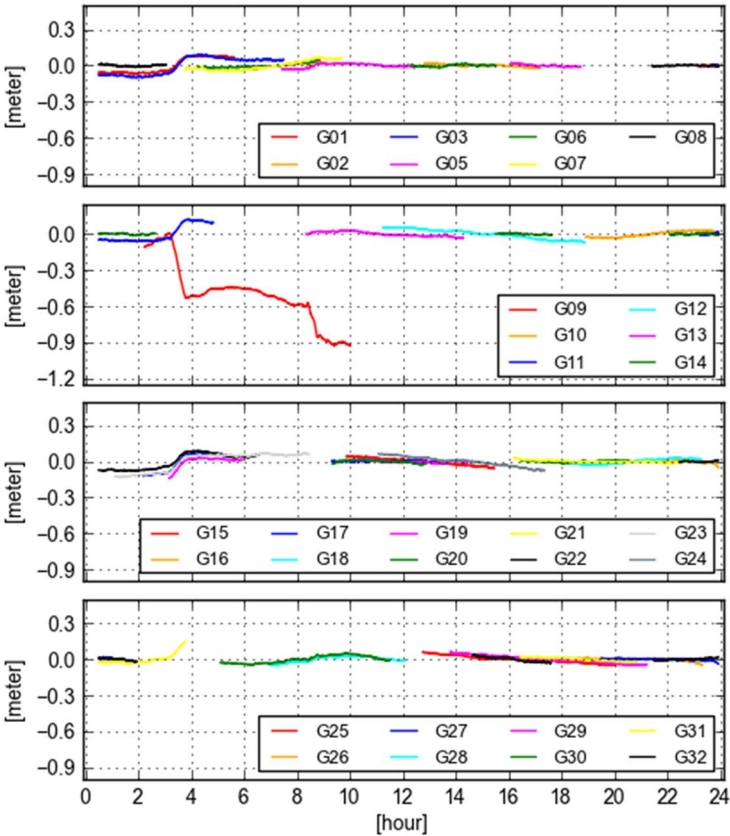
Figure 8. Variations of final orbit/clock and real-time orbit/clock differences projected into the LOS at Site KOKV for all visible GPS satellites

Figure 9 displays GB-GF WL ambiguities of PRN 09 computed with real-time orbit clock products for all selected sites. It is obvious that these time series are not stable. The figure discloses longer period of oscillations than one single site shown in figure 7. We could also see that the variation patterns are almost the same for some pairs of sites, e.g. KOKB and KOKV, KIRI and NAUR, MIZU and SANT, MRO1 and PERT. These pairs of sites have different observations, but demonstrate the same GB-GF WL patterns, as they suffer almost the same orbit clock error. It is clear in this case that the GB and GF WL ambiguities are not equivalent.

372
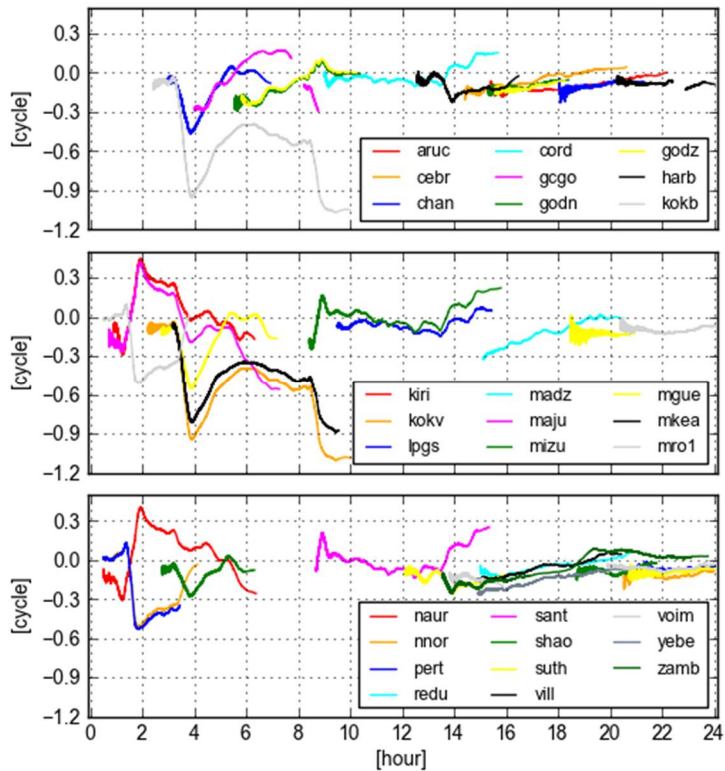
373   **Figure 9.** GB - GF WL ambiguities computed with real-time orbit clock products for GPS PRN 09 at
374   all selected sites

6. Simulation study of orbit/clock error effects

376   In order to further investigate the effects of orbit and clock errors on the WL ambiguities, we
377   simulate two types of errors directly in the LOS for one satellite of an entire tracking period at Site
378   KOKV: 1) a constant bias (e.g. 1.0 m); 2) time-variant errors with 0.15 m amplitude and 2 hours period
379   of sine or cosine changes. The errors are added to only PRN 30 of the ESA final orbit and clock. The
380   GB-GF WL ambiguities are then recomputed and compared with the previous ones. The purpose for
381   such a simulation is to see how effects of precisely known errors.
382   Figure 10 displays differences of recomputed GB-GF WL ambiguities with respect to their
383   counterparts without the simulated errors. The differences are purely caused by the simulated errors.
384   The top panel displays the GB-GF WL effects of a 1.0 m constant bias is added into the PRN 30 during
385   5:00 h – 11:30 h. The effect is about a constant bias of 0.084 cycle. There is no visible effects on other
386   satellites. This indicates that the GB-GF WL ambiguity is not very sensible to a constant bias, which
387   confirms the analysis in "orbit and clock residual error being constant bias".

388
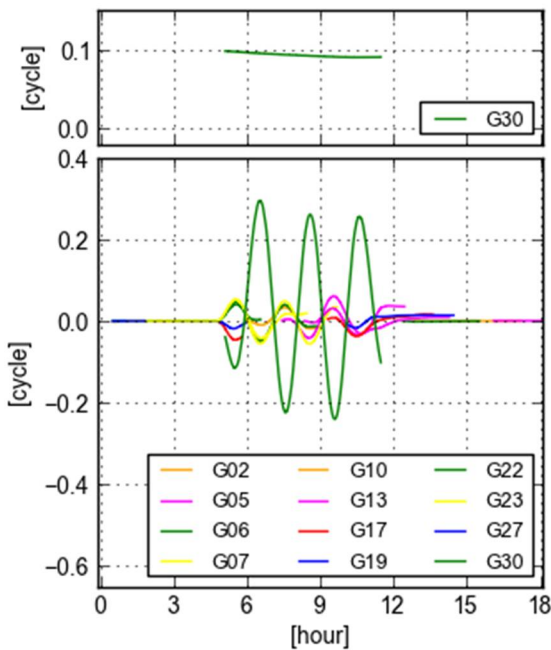
Figure 10. Recomputed GB-GF WL ambiguities minus the previous ones in figure 5 with the simulated constant bias (top) and the time-variant errors (bottom) added into orbit clock of PRN 30 at Site KOKV

The bottom panel demonstrates the GB-GF WL effects after the time-variant errors are added into the PRN 30 during 5:00 h – 11:30 h. Firstly, the effects of PRN 30 show also the sine or cosine behavior. Secondly, there are also similar patterns with smaller magnitude in many other satellites tracked in the same period. These effects are brought by the added errors with only 0.15 m in (absolute) size, which is much smaller than 1.0 m. This indicates that the GB-GF WL ambiguity is very sensible to time-variant errors as analyzed in "orbit and clock residual error being time-variant error", which provides an opportunity for real-time user to evaluate the quality of real-time orbit and clock.

7. Conclusions

This contribution derives L1, L2 and WL ambiguities from the GF and GB PPP model. Two types of orbit and clock products, represented different level of quality, are used to compute the WL ambiguities. The differences of GB and GF WL ambiguities are particularly analyzed. The main results and conclusions are summarized in the following.

The GF ambiguities are obtained on individual satellite basis, and there is no redundancy for the epoch-wise estimation. To improve GF estimates, multiple epochs of data are needed. The GB ambiguity estimation makes use of all received satellites, therefore the geometry and the redundancy, besides using multiple epochs of data, play roles on the estimation. From our implementation and experiment, there are significant differences between GB L1/L2 ambiguities and the GF ones in terms of both estimates and their precisions, however, the GB WL ambiguities do not differ much from the GF ones in terms of precision at least.

Orbit and clock have no impact on GF WL ambiguities as they are eliminated in the process, while they have effects on GB ones. Whether the GB and GF ambiguities are equivalent depends much on the quality of the used orbit and clock. In general, if GB-GF WL values are stably in between ± 0.1 cycles or within three times of their formal errors, we could state that the GB and GF WL ambiguities are equivalent. This is basically not an issue for the final orbit and clock product used in our experiment, as this type of product is obtained from post-processing.

The GB and GF WL ambiguities are not always equivalent if they are computed from the real-time orbit and clock, as the type of product is sometimes not perfect. It is found in this contribution

that the variation of GB-GF WL ambiguities are coincide with the orbit and clock differences between the final and real-time products. Therefore, it is promising for the real-time users that the GB-GF WL ambiguities can be directly used to indicate the orbit and clock quality from a user's perspective.

Two types of orbit and clock errors are simulated and the effects on GB-GF WL ambiguities are analyzed. The constant bias in orbit and clock seems not have significant effects on GB-GF WL values if we look into the pattern of their time-series, though there is still a smaller size of bias presenting. This indicates that the GB-GF WL ambiguity is not very sensible to a constant bias in orbit and clock. However, the GB-GF WL ambiguity varies remarkably if the time- variant errors exist in the orbit and clock. Even the errors are not large, it is sensitively mapped into GB-GF WL ambiguities. As this type of errors is more often showing up than the constant bias in the real-time orbit and clock, the GB-GF WL ambiguity provides an opportunity for real-time users to evaluate the quality of real-time orbit and clock.

Author Contributions: G.C. provided the initial concept and methodology; Q.Z. helped to derive the equations in theory with G.C.; G.C acquired the funding for the project and carried out the data processing. Q.Z. provided the software platform and results analysis. S.L. implemented the software part necessarily for this project and carried out the experimental validation; S.L. visualized the results and wrote the draft of the paper. G.C. and Q.Z. finalized the paper. All authors reviewed the paper.

Funding: This research was funded by the National Natural Science Foundation of China (Grant NO. 41674015, 41274035，41774036, 41574030).

Acknowledgments: The IGS is greatly acknowledged for providing GNSS raw data and precise orbit and clock.

Conflicts of Interest: The authors declare no conflict of interest.

References

1. Zumberge JF; Heflin MB; Jefferson DC; Watkins MM; Webb FH. Precise point positioning for the efficient and robust analysis of GPS data from large networks. *J Geophys Res* **1997**, *102(B3)*, pp.5005-5017, DOI:10.1029/96JB03860

2. Kouba J; Heroux P. Precise point positioning using IGS orbit products. *GPS Solut* **2001**,*5(2)*,pp.12–28

3. Geng J; Teferle FN; Shi C; Meng X; Dodson FN; Liu J. Ambiguity resolution in precise point positioning with hourly data. *GPS Solut* **2009**, *13(4)*, pp.263–270

4. Muellerschoen RJ; Iijima B; Meyer R; Bar-Server Y; Accad E. Real-time point-positioning performance evaluation of single-frequency receivers using NASA's global differential GPS system. Proceedings of ION GNSS 17th international technical meeting of the Satellite Division, 21-24 September 2004, Long Beach, CA, USA, pp.1874–1880

5. Leandro R et al. RTX positioning: the next generation of cm-accurate real-time GNSS positioning. Proceedings of the 24th International Technical Meeting of the Satellite Division of the ION, 20-23 September 2011,Portland Oregon, pp.1460-1475

6. Li X; Ge M; Dai X; Ren X. Accuracy and reliability of multi-GNSS real-time precise positioning: GPS, GLONASS, BeiDou, and Galileo. *J Geod* **2015,** *89(5)*, pp.607-635. DOI: 10.1007/s00190-015-0802-8

7. Ge M; Gendt G; Rothacher M; Shi C; Liu J. Resolution of GPS carrier phase ambiguities in precise point positioning (PPP) with daily observations. *J Geod* **2008**, *82(7)*, pp.389–399

8. Laurichesse D; Mercier F; Berthias JP. Zero-difference integer ambiguity fixing on single frequency receivers. Proceedings of ION ITM-2009, Anaheim, 26–28 January 2009, pp.2460–2469

9. Collins P; Bisnath S; Lahaye F; Heroux P. Undifferenced GPS ambiguity resolution using the decoupled clock model and ambiguity datum fixing. *Navigation* **2010**,*57(2)*, pp.123–135

10. Geng J; Shi C; Ge M; Dodson AH; Lou Y; Zhao Q; Liu J. Improving the estimation of fractional-cycle biases for ambiguity resolution in precise point positioning. *J Geod* **2012**,*86(8)*, pp.579–589

11. Li X; Li X; Yuan Y; Zhang K; Zhang X; Wickert J. Multi-GNSS phase delay estimation and PPP ambiguity resolution: GPS, BDS, GLONASS, Galileo. *J Geod* **2017**, DOI: 10.1007/s00190-017-1081-3

12. Wübbena G; Schmitz M; Bagge A. PPP-RTK: precise point positioning using state-space representation in RTK networks. Proceedings of ION GNSS 18th international technical meeting of the Satellite Division, The Institute of Navigation, Inc., September 2005, Fairfax, USA, pp.2584–2594

13. Teunissen PJG; Odijk D; Zhang B. PPP-RTK: results of CORS network-based PPP with integer ambiguity resolution. *Journal of Aeronautics Astronautics & Aviation* **2010**, *42(4)*, pp.223–230

14. Li X; Ge M; Zhang H; Wickert J. A method for improving uncalibrated phase delay estimation and ambiguity-fixing in real-time precise point positioning. *J Geod* **2013,** *87*, pp.405-416. DOI: 10.1007/s00190-013-0611-x

15. Chen G; Zhao Q. Near-field surface displacement and permanent deformation induced by the Alaska Mw 7.5 earthquake determined by high-rate real-time ambiguity-fixed PPP solutions. *Chin. Sci. Bull* **2014**, *59(34)*, pp.4781-4789. DOI: 10.1007/s11434-014-0609-7

16. Hatch R. The Synergism of GPS code and carrier measurements. Proceedings of the third international symposium on satellite Doppler positioning at physical sciences laboratory of New Mexico State University, 8-12 February 1982, *Vol. 2*, pp.1213-1231

17. Melbourne W. The case for ranging in GPS-based geodetic systems. Proceedings of First international symposium on precise positioning with the global positioning system,1985, Rockville, pp.373–386

18. Wübbena G. Software developments for geodetic positioning with GPS using TI-4100 code and carrier measurements. Proceedings of First international symposium on precise positioning with the global positioning system, 1985, Rockville, pp 403–412

19. Teunissen PJG; Khodabandeh A. Review and principals of PPP-RTK methods. *J Geod* **2015** *89(3)*, pp.217-240. DOI: 10.1007/s00190-014-0771-3

20. Montenbruck O et al. The multi-GNSS experiment (MGEX) of the international GNSS service (IGS) – Achievements, prospects and challenges. *Adv Space Res* **2017**, *59(7)*, pp.1671-1697

21. Kazmierski K; Sosnics K; Hadas T. Quality assessment of multi-GNSS orbits and clocks for real-time precise point positioning. *GPS Solut* **2018**, *22(1)*, pp.11. DOI: 10.1007/s10291-017-0678-6

22. Dilssner F; Springer T; Schoenemann; Zandbergen R; Enderle W. How GNSS spacecraft orientation error affect solar radiation pressure modelling. Presentation in EGU 2015, Vienna, Austria.

23. Kouba J. A simplified yaw-attitude model for eclipsing GPS satellites. *GPS Solut* **2009**, *13(1)*, pp.1-12

24. Lou Y; Zhang W; Wang C; Liu J. The impact of orbital errors on the estimation of satellite clock errors and PPP. *Adv Space Res* **2014**, *54(8)*, pp.1571-1580

25. Pan S; Chen W; Jin X; Shi X; He F. Real-time PPP based on the coupling estimation of clock bias and orbit error with broadcast ephemeris. *Sensors* **2015**, *15(7)*, pp.17808-17826; DOI:10.3390/s150717808

26. Khodabandeh A; Teunissen PJG. An analytical study of PPP-RTK corrections: precision, correlation and user-impact. *J Geod* **2015**, *89(11)* pp.1109-1132. DOI: 10.1007/s00190-015-0838-9